

Dinuclear Ruthenium Complexes Bearing Dicarboxylate and Phosphine Ligands. Acceptorless Catalytic Dehydrogenation of 1-Phenylethanol

Jeroen van Buijtenen,[†] Jan Meuldijk,[‡] Jef A. J. M. Vekemans,[†] Lambertus A. Hulshof,^{*,†} Huub Kooijman,[§] and Anthony L. Spek[§]

Laboratory of Macromolecular and Organic Chemistry, Eindhoven University of Technology, P.O. Box 513, 5600 MB Eindhoven, The Netherlands, Process Development Group, Eindhoven University of Technology, P.O. Box 513, 5600 MB Eindhoven, The Netherlands, Bijvoet Center for Biomolecular Research, Crystal and Structural Chemistry, Utrecht University, Padualaan 8, 3584 CH, Utrecht, The Netherlands

Received September 12, 2005

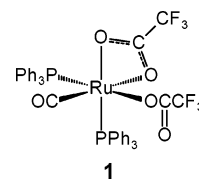
Reaction of $\text{RuH}_2\text{CO}(\text{PPh}_3)_3$ with tetrafluorosuccinic acid at 100 °C gave rise to the formation of the dinuclear bis(tetrafluorosuccinate)-bridged Ru(II) complex **2**, containing two water ligands. Exchange of the PPh_3 in complex **2** with various diphosphine ligands afforded a series of analogous complexes **3**. Reaction of the latter with 1-phenylethanol at 130 °C or with 2-propanol/ Et_3N at room temperature furnished the dinuclear dihydrido-bridged Ru(II) complexes **4**. Complexes **2** and **4** were characterized by X-ray diffraction analysis. Both bis(tetrafluorosuccinate)-bridged complexes **3** and dihydrido-bridged complexes **4** catalyze the acceptorless dehydrogenation of 1-phenylethanol to acetophenone and dihydrogen with good yields and excellent selectivity under relatively mild conditions in the absence of acid or base. A tentative catalytic cycle for the dehydrogenation of secondary alcohols by Ru(II) complexes of type **3** is presented.

Introduction

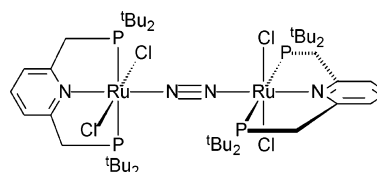
The development of catalytic oxidations of alcohols under mild reaction conditions is highly appealing because of its industrial significance. The importance of environmental acceptability of processes has led to much effort in the development of sustainable technologies. Important criteria include high atom efficiency, formation of little (in)organic waste, use of acceptable solvents, and selective synthesis of the desired products.¹

Various catalytic systems have been developed to meet these criteria, using environmentally acceptable oxidants such as hydrogen peroxide, molecular oxygen, and to a lesser extent sodium hypochlorite.² Nevertheless, the highest possible atom efficiency is achieved in acceptorless dehydrogenation of secondary alcohols to yield ketones along with dihydrogen as the sole byproduct. Homogeneous catalysts for this reaction are relatively rare, but the conversion was successfully achieved with $\text{Rh}(\text{III})\text{-SnCl}_2/\text{HCl}$,³ $\text{Rh}(\text{OAc})_4/\text{PR}_3$,⁴ and $\text{Ru}(\text{OCOCF}_3)_2\text{-}(\text{CO})(\text{PPh}_3)_2/\text{CF}_3\text{COOH}$ (**1**).^{5–7} However, using these catalysts a catalytic amount of acid is still required as a hydride ion acceptor.

Scheme 1



Scheme 2



Moreover, most of these catalysts were investigated with the aim to produce hydrogen gas from simple alcohols, and the concomitant conversion of secondary alcohols into ketones was not thoroughly investigated. More recently, Choi et al. reported on an immobilized form of Shvo's well-known hydroxycyclopentadienyl Ru(II) catalyst,⁸ which catalyzed the dehydrogenation of secondary alcohols in good yields without any additives, although a high metal loading was required. Finally, Zhang et al. reported on a ruthenium complex bearing a *t*-Bu-PNP pincer ligand (Scheme 2) that, after activation by a base, also catalyzed this reaction with good yield and selectivity, without the need for further additives.⁹ Recently, the same group reported on complexes bearing similar PNP and PNN pincer

* To whom correspondence should be addressed. E-mail: l.a.hulshof@tue.nl. Phone: +31 40 2473134. Fax: +31 40 2451036.

[†] Laboratory of Macromolecular and Organic Chemistry, Eindhoven University of Technology.

[‡] Process Development Group, Eindhoven University of Technology.

[§] Utrecht University.

(1) Hoelderich, W. F. *Catal. Today* **2000**, *62*, 115.

(2) (a) Sheldon, R. A.; van Santen, R. A. *Catalytic oxidation: principles and applications*; World Scientific: Singapore, 1995. (b) Sheldon, R. A.; Arends, I. W. C. E.; Ten Brink, G.-J.; Dijkman, A. *Acc. Chem. Res.* **2002**, *35*, 774. (c) Bäckvall, J.-E. *Modern oxidation methods*; Wiley VCH: Weinheim, 2004.

(3) Charman, H. B. *J. Chem. Soc. B* **1970**, *4*, 584.

(4) Shinoda, S.; Kojima, T.; Saito, Y. *J. Mol. Catal.* **1983**, *18*, 99.

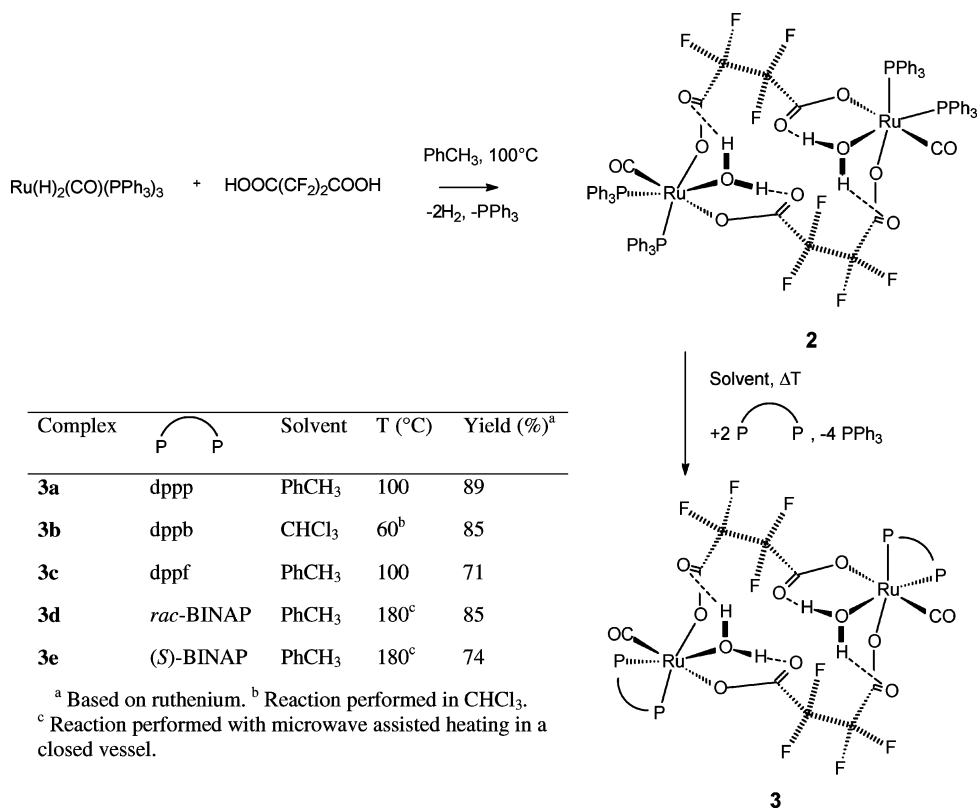
(5) Dobson, A.; Robinson, S. D. *J. Organomet. Chem.* **1975**, *87*, C52.

(6) Dobson, A.; Robinson, S. D. *Inorg. Chem.* **1977**, *16*, 137.

(7) Jung, C. W.; Garrou, P. E. *Organometallics* **1982**, *1*, 658.

(8) Choi, J. H.; Kim, N.; Shin, Y. J.; Park, J. H.; Park, J. *Tetrahedron Lett.* **2004**, *45*, 4607.

Scheme 3



ligands that efficiently and selectively catalyze dehydrogenation of primary alcohols to esters and H₂.¹⁰

Previously, we reported on the application of ruthenium complex **1** as a catalyst for the acceptorless catalytic dehydrogenation of secondary alcohols.¹¹ Various aliphatic alcohols could be dehydrogenated with unprecedented results regarding yield and selectivity. However, the catalytic amount of trifluoroacetic acid (TFA) that is required for the activity and stability of the catalyst, combined with the high reaction temperature, led to significant formation of byproducts, especially in the case of benzylic substrates. Indeed, considerable amounts of 1-phenylethyl trifluoroacetate and di(1-phenylethyl)ether could be detected in the catalytic dehydrogenation of 1-phenylethanol. Here, we report on novel tetrafluorosuccinic acid (TFSA) analogues of **1** not requiring additional acid. With these complexes, high activity and excellent selectivity were observed in the acceptorless dehydrogenation of 1-phenylethanol.

Results and Discussion

Synthesis and Characterization of [Ru(μ -OCO-C₂F₄-OCO)(CO)(H₂O)(PPh₃)₂]₂, **2.** It was expected that substitution of the trifluoroacetate ligands in **1** by a bifunctional perfluorocarboxylate might lead to a catalytically active Ru complex that is more stable and more reactive than **1**. Furthermore, an excess of TFA would no longer be required using such a catalyst. Therefore, in analogy to the synthesis of **1**,¹² Ru(H)₂(CO)(PPh₃)₃

was reacted with TFSA, followed by aqueous workup, resulting in the formation of dinuclear complex **2** (Scheme 3).¹³

³¹P{¹H} NMR of **2** reveals two sharp doublets (²J_{PP} = 29.2 Hz) at 43.6 and 40.8 ppm, which can be assigned to two nonequivalent triphenylphosphine ligands. The observation of these sharp signals at room temperature is in contrast with the ³¹P{¹H} NMR of **1**, which exhibits one broad signal at approximately 40 ppm for the triphenylphosphine ligands, presumably indicative of fast exchange between mono- and bidentate coordination of the two carboxylate ligands. At 220 K an AB pattern similar to that of **2** can be observed in the ³¹P{¹H} NMR spectrum of **1**.¹⁴ Obviously, **2** lacks the dynamics of the TFA complex **1** at room temperature, which can be attributed to the hydrogen bonding that is observed between the protons of the water ligands and the carbonyl oxygens of the tetrafluorosuccinate (vide infra). In accordance with the apparent rigidity of complex **2**, ¹⁹F NMR reveals four signals ranging from -123 to -118 ppm for the four different fluorine nuclei present in the two equivalent tetrafluorosuccinate ligands. The geminal coupling constants are approximately 270 Hz. In ¹H NMR a typical broad signal attributed to the two symmetrical water ligands is observed at 6.32 ppm. ¹³C{¹H} NMR reveals an unresolved triplet for the Ru-CO at 202.7 ppm as well as two unresolved triplets at 165.9 and 169.0 ppm, which can be assigned to the carbonyls of the tetrafluorosuccinate ligand.

Yellow prismatic crystals of **2** suitable for X-ray diffraction analysis were grown by slow diffusion of *n*-pentane into a solution of the complex in toluene/chloroform (1:1) at room

(9) Zhang, J.; Gandelman, M.; Shimon, L. J. W.; Rozenberg, H.; Milstein, D. *Organometallics* **2004**, *23*, 4026.

(10) Zhang, J.; Leitus, G.; Ben-David, Y.; Milstein, D. *J. Am. Chem. Soc.* **2005**, *127*, 10840.

(11) Ligthart, G. B. W. L.; Meijer, R. H.; Donners, M. P. J.; Meuldijk, J.; Vekemans, J. A. J. M.; Hulshof, L. A. *Tetrahedron Lett.* **2003**, *44*, 1507.

(12) Dobson, A.; Robinson, S. D.; Uttley, M. F. *J. Chem. Soc., Dalton Trans.* **1975**, 370.

(13) Synthesis of analogous complexes with perfluoroglutaric acid or succinic acid yielded intractable solids, which were not further investigated. A complex analogous to **2** with two 2,2-difluorosuccinic acid ligands was successfully synthesized, but catalytic performance was inferior to that of the perfluorosuccinic acid complex.

(14) Creswell, C. J.; Dobson, A.; Moore, D. S.; Robinson, S. D. *Inorg. Chem.* **1979**, *18*, 2055.

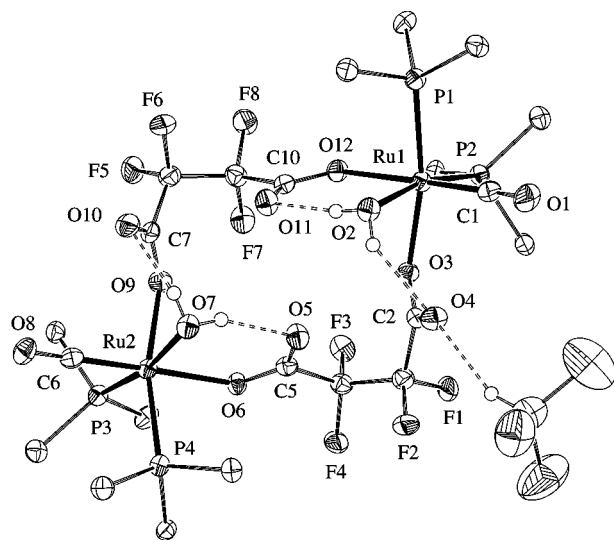


Figure 1. ORTEP plot²⁹ at 50% probability level of the molecular structure of **2**. For reasons of clarity, hydrogen atoms not involved in hydrogen bonding have been omitted and the P–Ph groups are represented as P–C.

temperature. The molecular structure of **2** is displayed in Figure 1. The existence of hydrogen bonds between the coordinated water and acid moieties is confirmed by the donor...acceptor distances O2...O4 = 2.822(4) Å, O2...O11 = 2.591(3) Å, O7...O5 = 2.623(4) Å, and O7...O10 = 2.733(3) Å. The structure contains an ordered chloroform solvent molecule, which is involved in a C–H...O interaction with O4; see Figure 1. The complex is apparently strongly stabilized by hydrogen bonding between the protons of the water ligands and the carboxylate oxygens. ¹H NMR reveals that the water ligands in **2** are readily displaced by alcohols (both primary and secondary).

Synthesis and Characterization of Diphosphine Complexes [Ru(μ-OCO-C₂F₄-OCO)(CO)(H₂O)(P–P)]₂, **3a–e.** Reaction of complex **2** with a slight excess of a diphosphine at elevated temperature gave diphosphine complexes **3a–e** (Scheme 3).

Generally, the reactions proceeded in good yield, and the resulting diphosphine complexes were isolated by crystallization.¹⁵ This straightforward ligand exchange in dinuclear complex **2** is in sharp contrast with the efforts required for achieving an analogous substitution in the mononuclear complex **1**.⁷ Direct exchange of the triphenylphosphine ligands in **1** proved to be impossible and resulted in an ill-defined mixture of products. The same substitution could only be achieved, albeit in moderate yield, by exchange of PPh₃ with the diphosphine in its precursor, RuH₂(CO)(PPh₃)₃. It is reasonable to assume that the markedly higher rigidity and stability of complex **2** compared to complex **1** are responsible for the difference in behavior toward ligand substitution. This renders complex **2** an ideal platform for the synthesis of a series of phosphine bearing bis(tetrafluorosuccinate)-bridged ruthenium catalysts.

Whereas exchange of PPh₃ was easily accomplished with dppp, dppb, and dppf (Scheme 3), this did not hold for *rac*-BINAP. The reaction was not complete after 24 h, even at 130 °C in *p*-xylene. Since such conditions were not desirable, the reaction was attempted with microwave-assisted heating (Scheme 3). During a period of 80 min at 180 °C in toluene, under elevated pressure, complete conversion to and precipitation of ruthenium complex **3d** from the reaction mixture occurred. The reaction of **2** with (*S*)-BINAP was performed under similar

conditions, resulting in complete conversion and a clear yellow solution. Complex **3e** was obtained in good yield after recrystallization.

³¹P{¹H} NMR of **3a–e** reveals two doublets for the two nonequivalent phosphorus atoms, similar to **2**. In ¹⁹F NMR geminal coupling is again observed for the fluorine nuclei of the two equivalent tetrafluorosuccinic acid ligands, and in ¹H NMR the protons of the water ligand appear as a broad signal at approximately 6 ppm. The spectral similarity with compound **2** suggests a similar dinuclear structure with bridging tetrafluorosuccinate for **3a–e**. For the (*rac*)-BINAP complex **3d** signals for the two possible diastereomers are observed in ¹H, ¹³C{¹H}, ¹⁹F{¹H}, and ³¹P{¹H} NMR. The major compound (>80%) exhibits the same signals as the (*S*)-BINAP complex and can therefore be assigned to (*R,R*)- and (*S,S*)-**3d**. Overlapping signals and a low relative concentration prevented the determination of the exact chemical shift and coupling in the NMR spectra of the (*R,S*)-**3d** diastereomer.

Reaction of **3e with 1-Phenylethanol. Formation of the Dinuclear Ruthenium Hydride Complex [Ru(μ-H)(μ-OCO-C₂F₄-OCO)(CO)((*S*)-BINAP)]₂·2H₂O, **4e**.** When **3a–e** are heated to 130 °C in the presence of 1-phenylethanol, dehydrogenation of the alcohol is observed and a new complex is quickly formed, accompanied by a color change. After dehydrogenation of 1-phenylethanol with **3d** and **3e**, the new complexes that are formed during catalysis have been isolated as air-stable orange solids **4d** and **4e**, respectively (Scheme 4). In a separate experiment, the dinuclear hydride complex **4e** was also obtained in high yield by reaction of **3e** with 500 equiv of 2-propanol and 250 equiv of triethylamine in toluene at 25 °C in an argon atmosphere.¹⁶ The structure of **4d** and **4e** was unequivocally assigned with the aid of NMR and X-ray diffraction analyses of the product.

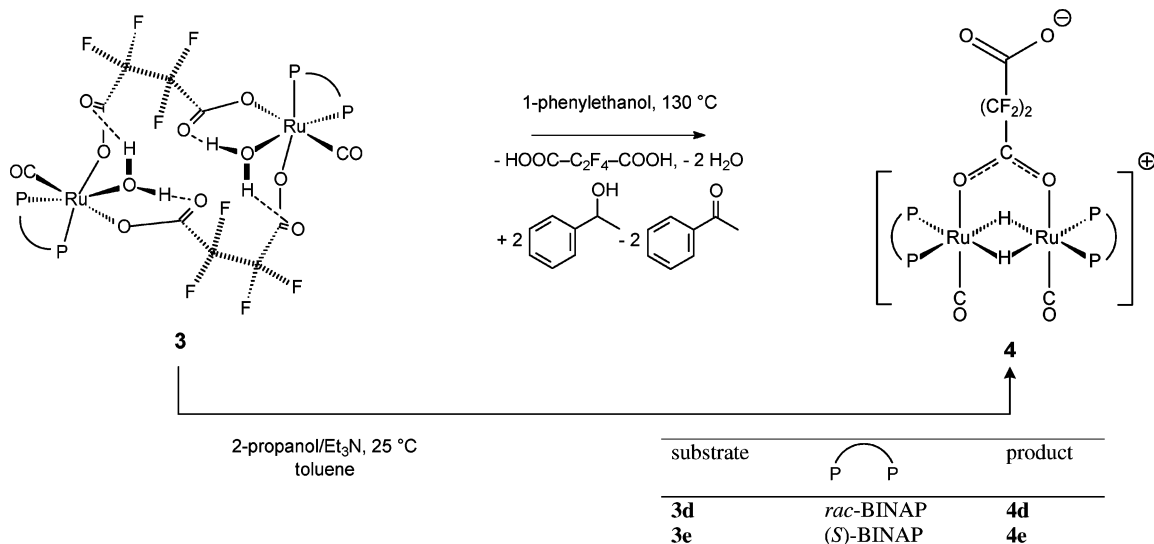
In the ¹H NMR spectrum of **4e** a triplet of triplets appears in the hydride region at –10.38 ppm (²J_{HP}(trans) = 48.0 Hz, ²J_{HP}(cis) = 10.0 Hz). Integral values suggest two hydride ligands per dinuclear complex. These observations can be rationalized by adopting two equivalent bridging hydrides in a dinuclear complex that couple with two trans ³¹P nuclei atoms and two cis ³¹P nuclei. Apparently, the nonequivalence of the geminal phosphorus atoms on the same ruthenium center due to the chiral (*S*)-BINAP ligand does not have a significant effect on the coupling with the hydrides. The ³¹P{¹H} NMR spectrum reveals two double doublets at 38.8 and 46.3 ppm with ²J_{PP} = 36.0 Hz and ⁴J_{PP} = 26.1 Hz. This coupling originates from the nonequivalence of the geminal phosphorus atoms (vide supra), and a significant ⁴J_{PP} is observed. This is in agreement with long-range phosphorus–phosphorus coupling reported for similar hydride-bridged dinuclear complexes.¹⁷ In ¹⁹F NMR four doublets are observed for the four nonequivalent fluorine nuclei with geminal couplings of 271 Hz. The ¹³C NMR spectrum reveals an unresolved triplet at 203.5 ppm due to the two equivalent Ru–CO groups and two unresolved triplets at 161.9 and 164.4 ppm assigned to the two carbonyls of the tetrafluorosuccinic acid ligand. One tetrafluorosuccinic acid ligand bridges the ruthenium nuclei as a carboxylate, and the uncoordinated carboxylate acts as the counterion for the overall positive charge of the two ruthenium(II) centers. The NMR spectra of **4d** are more complicated, due to the presence of signals for both diastereomers of the dinuclear (*rac*)-BINAP

(16) **4e** was isolated as a trihydrate as judged from ¹H NMR and elemental analysis.

(17) (a) Bianchini, C.; Barbaro, P.; Scapacci, G.; Zanobini, F. *Organometallics* **2000**, *19*, 2450. (b) Tani, K.; Iseki, A.; Yamagata, T. *Chem. Commun.* **1999**, 1821.

(15) **3b** and **3c** were isolated as a complex containing an extra molecule of mobile water as judged from ¹H NMR and elemental analysis.

Scheme 4



complex. However, the combination of NMR data and X-ray diffraction analysis of an isolated crystal (see Supporting Information) confirms a similar dinuclear structure with two bridging hydrides for (*R,S*)-**4d**.

The structure assigned to dihydrido-bridged complexes **4** implies the loss of one of the tetrafluorosuccinic acid ligands during the reaction. The hydride ligands should originate from the dehydrogenation of 2 equiv of alcohol, since ruthenium remains divalent. The second tetrafluorosuccinic acid ligand of the precursor is lost either as the reprotoneated diacid in the reaction with 1-phenylethanol at 130 °C or as its triethylamine salt in the reaction with triethylamine. In the dehydrogenation at elevated temperature this trace of carboxylic acid may be responsible for the formation of a trace amount of byproduct.

Orange crystals of **4d** suitable for X-ray diffraction analysis could be obtained, and depending on the chosen conditions, either triclinic or monoclinic crystals were grown. Slow diffusion of *n*-pentane into a solution of the complex in dichloromethane resulted in the formation of the triclinic crystals, while crystallization from methanol yielded the monoclinic crystals. The triclinic crystals contain two independent molecules of (*R,R*)-**4d** (Figure 2). Since they crystallize in the centrosymmetric space group $P\bar{1}$ the unit cell contains a racemic mixture of (*R,R*)-**4d** and (*S,S*)-**4d**. This form will be referred to as (*rac*)-**4d** throughout this paper. The monoclinic crystals are of (*R,S*)-**4d**

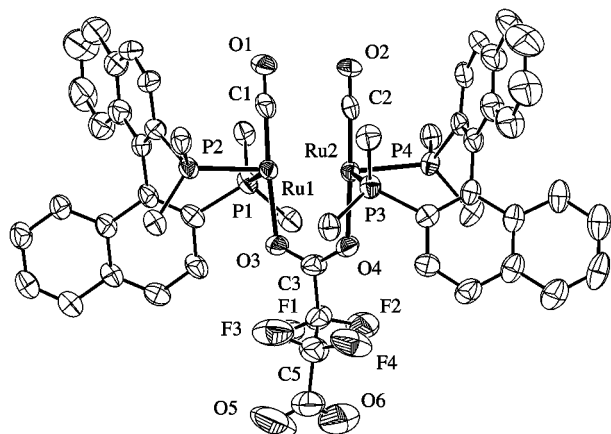


Figure 2. ORTEP plot²⁹ at 50% probability level of the molecular structure of (*rac*)-**4d**. For reasons of clarity, hydrogen atoms have been omitted and the P-Ph groups are represented as P-C.

and also have a centrosymmetric space group (see Supporting Information). The bridging hydrides could not be resolved in the crystal structure, but their presence was secured by ¹H NMR. The distance between the two ruthenium centers is 2.7270(19) Å in (*R,S*)-**4d** and 2.711(8) and 2.7205(9) Å in the two independent molecules of (*rac*)-**4d**. These distances are in the range observed for dihydrido-bridged ruthenium dimers (2.47–3.03 Å) included in the Cambridge Structural Database (Version 5.26 of November 2004, updates 1 and 2 installed).¹⁸ This configuration would lead to an 18-electron configuration around both metal atoms, which is in agreement with its high stability. However, the distance between the ruthenium centers does not, by itself, exclude the possibility of a single hydride-bridged dimer (observed in the CSD: 2.59–3.23 Å) or a Ru–Ru bond (observed in the CSD: 2.17–3.38 Å). The C–O bond distances of the uncoordinated side of the tetrafluorosuccinate ligand suggest deprotonation, which is in agreement with the fact that the free side of the ligand acts as the counterion for the overall positive charge of the complex.¹⁹

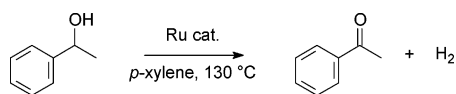
A similar ruthenium complex, [(Ph₃P)₄Ru₂(μ-H)₂(μ-CF₃-SO₂)(CO)₂]HC(SO₂CF₃)₂, was reported by Siedle et al.²⁰ The two bridging hydrides as well as the bridging trifluoromethanesulfinate ligand are similar to the structure proposed for **4**, while HC(SO₂CF₃)₂[−] acts as the counterion. Furthermore, the complex featured four equatorial triphenylphosphine ligands. NMR data (¹H and ³¹P) for this complex, for which the structure was confirmed by X-ray diffraction analysis, are similar to the spectral data for **4e**.

Dehydrogenation of 1-Phenylethanol. Heating 1-phenylethanol with 0.2 mol % of complexes **2** or **3a–e** in *p*-xylene at 130 °C in an argon atmosphere resulted in dehydrogenation with the concomitant evolution of dihydrogen (Table 1). To allow for reproducible conditions, the catalyst and the reactants were first heated to 130 °C without solvent, which gives rise to very fast formation of the hydride-bridged dinuclear complex **4**, after which *p*-xylene was added. The reactions are clearly not first-order in the substrate concentration, and product inhibition

(18) Allen, F. H. *Acta Crystallogr., Sect. B: Struct. Sci.* **2002**, *58*, 380.

(19) The difference between both C–O bond lengths is 0.00 ± 0.02 and 0.009 ± 0.011 Å for both complexes in the unit cell of (*rac*)-**4d** and 0.12(4) Å for (*R,S*)-**4d**.

(20) (a) Siedle, A. R.; Newmark, R. A.; Pignolet, L. H. *Inorg. Chem.* **1986**, *25*, 1345. (b) Siedle, A. R.; Newmark, R. A.; Korba, G. A.; Pignolet, L. H.; Boyle, P. D. *Inorg. Chem.* **1988**, *27*, 1593.

Table 1. Dehydrogenation of 1-Phenylethanol at 130 °C Using Various Catalysts^a

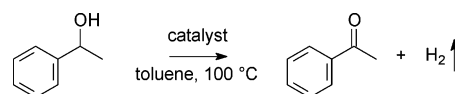
entry	cat.	[cat.] (mol %)	conv (%)		yield (%)		TON 24 h
			5 h	24 h	5 h	24 h	
1 ^b	1	0.4	21	35	17	29	72
2	2	0.2	14	21	13	20	50
3	3a	0.2	33	79	33	79	197
4	3b	0.2	45	71	45	71	178
5 ^c	3c	0.2	48	76	48	76	191
6 ^c	3c	0.1	45	70	45	70	350
7	3c	0.025	27	34	27	34	651
8	3d	0.2	53	81	53	81	203
9 ^c	3e	0.2	40	63	40	63	145
10 ^{c,d}	4d	0.2	35	56	35	56	132
11 ^{c,d,e}	4d	0.2	34	62	34	62	152

^a Reaction conditions: 5 mmol of 1-phenylethanol, 0.25 mmol of 1,3,5-tri-*tert*-butylbenzene (internal standard); 2.5 mL of *p*-xylene; heated at 130 °C for 24 h under an argon atmosphere in an open system. ^b 0.24 mmol of TFA. ^c Catalyst is not completely dissolved during reaction. ^d Final conversion is given after 22 h instead of 24 h. ^e 1.5 equiv of TFSA was added to the reaction.

appears to limit the rate of reaction at higher conversions. As a reference the reaction was performed using Ru complex **1** with 12 equiv of TFA as the catalyst (Table 1, entry 1). A significant amount of byproducts, predominantly 1-phenylethyl trifluoroacetate and di(1-phenylethyl)ether, were formed under these strongly acidic conditions. Byproduct formation was markedly reduced when using the dinuclear Ru complex **2** as the catalyst (Table 1, entry 2). However, this complex was clearly not very stable under the reaction conditions since the activity toward dehydrogenation of 1-phenylethanol quickly decreased. Moreover, due to apparent decomposition of the catalyst, a small amount of byproduct was still formed.

The bidentate phosphine complexes **3a–d** (Table 1, entries 3–8) performed much better: no catalyst decomposition and accompanying byproduct formation could be observed, and the dehydrogenation activity was superior to complexes **1** and **2**. The best results were obtained using complexes **3c** and **3d**. Remarkably, the solubility of the catalyst in the reaction medium is very limited in the case of the dppe complex **3c**. With 0.2 mol % of **3c**, part of the catalyst remained undissolved. This prompted us to repeat the reaction with lower concentrations of the catalyst (Table 1, entries 6 and 7). The drop in conversion was clearly not proportional to the lower catalyst loading, and a high TON of 651 for this reaction could be reached after 24 h using 0.025 mol % of **3c**, a catalyst loading guaranteeing a homogeneous reaction mixture. The reaction with bidentate complexes **3a–e** eventually reaches complete conversion, and using 0.2 mol % of (*rac*)-BINAP complex **3d** a conversion of 92% was achieved after 48 h, corresponding to a TON of 230. Interestingly, no additives are required for this catalyst, and it is active under relatively neutral conditions. This is in marked contrast to most other catalytic alcohol dehydrogenation catalysts, which require either excess base or acid (*vide supra*). Consequently, acid- or base-promoted byproduct formation is prevented when using the complexes **3a–e**.

When using the chiral (*S*)-BINAP catalyst **3e** (Table 1, entry 9), a slight enantioselectivity for the dehydrogenation of (*R*)-1-phenylethanol could be observed. However, the enantiomeric excess of the remaining substrate never surmounted 4%, and after 5 h of reaction the unconverted substrate was again nearly racemic. This suggests that the enantioselectivity of the reaction

Table 2. Dehydrogenation of 1-Phenylethanol at 100 °C Using Various Catalysts^a

entry	cat.	[cat.] (mol %)	TOF (h ⁻¹)	time (h)	conv (%)	yield (%)	TON ^b
1	3a	0.5	1.2	73	46	46	45
2	3b	0.5	3.8	121	93	93	94
3 ^c	3c	0.5	3.5	92	93	93	92
4 ^c	3c	0.25	7.1	117	92	92	187
5 ^c	3c	0.1	19.4	117	79	79	383
6	3e	0.5	3.3	92	93	93	96
7	2	0.5	5.1	21	36	36	35

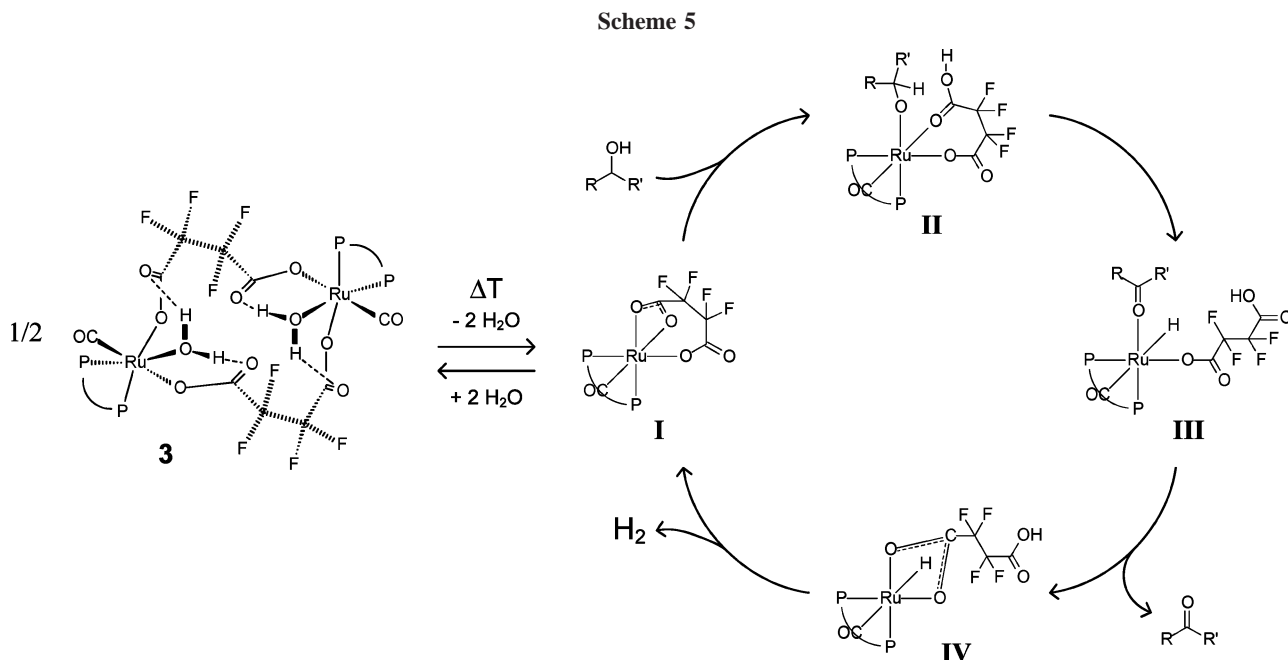
^a Reaction conditions: 0.5 mmol of 1-phenylethanol, 0.025 mmol of 1,3,5-tri-*tert*-butylbenzene (internal standard); 0.5 mL of toluene; reaction at 100 °C under an argon atmosphere in an open system. ^b Turnover frequency: mol of 1-phenylethanol converted (mol of Ru)⁻¹ h⁻¹; calculated over the first 24 h. ^c Catalyst is not completely dissolved during reaction.

is limited and that racemization is fast under these reaction conditions. The activity of **3e** was slightly lower than that of the (*rac*)-BINAP catalyst **3d**, presumably due to the absence of the more active *meso*-catalyst.²¹

Isolated dihydrido-ruthenium complex **4d** was also applied as a catalyst in the dehydrogenation of 1-phenylethanol (Table 1, entry 10). Although the catalyst was not completely dissolved, the observed rate of reaction is of the same order of magnitude as that for the reaction with **3d**. Therefore, **4d** appears to be a resting state in the catalytic cycle. In another experiment **4d** was used as the catalyst along with 1.5 equiv of free tetrafluorosuccinic acid (Table 1, entry 11). However, this did not affect the rate of reaction. Since the activity of **4d** is comparable to that of **3d** and since addition of tetrafluorosuccinic acid to dehydrogenation with **4d** does not enhance the rate of reaction, free carboxylic acid does not seem to play a crucial role in the catalytic cycle.

Interestingly, when the reaction was performed at 100 °C, it was first-order in substrate concentration (Table 2). Formation of the dinuclear ruthenium hydride complex **4** is very slow and almost inhibited: when using (*S*)-BINAP complex **3e** as the catalyst, approximately 25% of the complex is converted to **4e** and the rest is recovered as **3e** upon workup of the reaction mixture after 92 h, as evidenced by ³¹P{¹H} NMR. Decomposition of the catalyst is negligible. With the dppe complex **3c** a similarly slow conversion of the complex into the dinuclear ruthenium hydride is observed, while solubility of the catalyst in the reaction medium is very limited (Table 2, entry 3). Therefore, the reaction was repeated at catalyst loadings of 0.25 and 0.1 mol % (Table 2, entries 4 and 5). As expected, this induced a proportional increase of the turnover frequency (TOF). However, at lower catalyst loadings an increasing deviation from first-order kinetics is observed (see Supporting Information). This can be rationalized by the formation of less active **4c**, which is buffered by undissolved **3c** at higher catalyst loadings. At a loading of 0.1 mol % of **3c**, when the catalyst is almost completely dissolved, a high initial TOF of 19.4 h⁻¹ and a TON of 383 could be achieved. Again, no significant enantioselectivity was observed using the chiral (*S*)-BINAP catalyst **3e** (Table 2, entry 6). Using complex **2** a TOF of 5.1 h⁻¹ was achieved (Table 2, entry 7). However, the stability of this catalyst was

(21) The batch of catalyst **3d** that was used for dehydrogenation was synthesized using conventional heating, and this resulted in an approximately 1:1 ratio of (*rac*)-**3d** vs (*R,S*)-**3d**.



again limited and high conversions could not be reached, in contrast to dehydrogenation catalyzed by **3b**, **3c**, and **3e**.²²

The behavior of PPh_3 complex **2** was studied at elevated temperature by VT-NMR (see Supporting Information). In $^{31}\text{P}\{^1\text{H}\}$ NMR, not only did the two characteristic doublets coalesce at higher temperature, but apparently another more flexible complex is formed, judged from the appearance of a broad signal at 44.0 ppm, which is shifted downfield from the center of the two original doublets (at 40.2 and 45.4 ppm). It is reasonable to assume that at these temperatures the water ligands are released and a mononuclear complex similar to complex **1** is formed. The original TFSA-bridged dinuclear complex **2** was recovered upon cooling to room temperature. VT-NMR of complex **2** was then performed in the presence of 1-phenylethanol (Figure 3). Coalescence is again observed at elevated temperatures, but now a different complex is formed in the end, exhibiting a signal at 43.1 ppm. This complex is apparently a hydride complex, as it also exhibits a (broad) signal at -16.7 ppm.²³ Upon cooling to room temperature, this complex is partly converted into the original dinuclear complex **2**, while approximately half of the hydride complex remains. In $^{19}\text{F}\{^1\text{H}\}$ NMR two broad signals are observed at -123.8 and -119.2 ppm. The hydride complex quickly decomposes upon exposure to air.

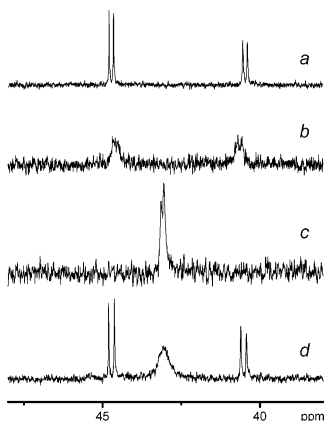


Figure 3. $^{31}\text{P}\{^1\text{H}\}$ NMR spectra of complex **2** in the presence of 107 equiv of 1-phenylethanol in *d*-toluene at (a) 25 °C, (b) 60 °C, and (c) 100 °C and (d) after cooling to 25 °C.

Considering the formation of these apparently mononuclear complexes under the reaction conditions and assuming catalytic behavior similar to the original TFA complex **1**, a tentative catalytic cycle for the dehydrogenation of secondary alcohols by bis(tetrafluorosuccinate)-bridged complex **3** is presented in Scheme 5.^{6,7} At elevated temperature the dimer is assumed to be split into two mononuclear complexes **I**, both with one tridentate TFSA ligand. Coordination of an alcohol and subsequent transfer of its proton to the TFSA ligand will lead to the formation of complex **II**, in which one of the carboxylate functions of the TFSA ligand is converted to a carboxylic acid function. β -Hydride elimination produces a hydride ligand and a coordinated ketone, while the carboxylate function of the TFSA ligand coordinates to the ruthenium with the carboxylic acid function uncoordinated (**III**). This is in contrast to the proposed catalytic cycle for the TFA complex **1**, in which one of the two TFA ligands is released, necessitating an excess of acid and creating highly acidic reaction conditions. Loss of the weakly coordinated ketone results in the formation of complex **IV**. Attack of the carboxylic acid function in complex **IV** on the hydride would then liberate molecular hydrogen and restore the active catalyst **I**. The formation of dihydride-bridged complex **4** is the result of a side reaction, which, depending on the reaction conditions, can be suppressed. For the dehydrogenation results at 130 °C, presented in Table 1, fast formation of **4** was ensured. In that case the reaction involves a different, unknown, catalytic cycle.

Summary

A range of novel dinuclear ruthenium dicarboxylate complexes has been synthesized. Both bis(tetrafluorosuccinate)-bridged complexes **3** and dihydride-bridged complexes **4** are highly stable and have been fully characterized. These complexes catalyze the acceptorless catalytic dehydrogenation of

(22) Complex **3d** was screened as well. Despite the presence of $\sim 80\%$ of the racemic isomer, its low solubility—in contrast to that of optically pure **3e**—prevented efficient dehydrogenation.

(23) This does not correspond with the position of the hydride signals for the PPh_3 complex analogous to **4**. While we were unable to isolate this complex, a triplet of triplets at -12.0 ppm in ^1H NMR in CDCl_3 could be observed for the bridging hydride ligands.

1-phenylethanol with good yield and high selectivity under relatively mild conditions: no additives are required and the catalyst is active under neutral conditions. High turnover numbers up to 543 after 5 h have been achieved using the ferrocene complex **3c**. A tentative catalytic cycle for the acceptorless dehydrogenation of secondary alcohols by complexes **3a–e** has been presented. We are currently investigating the scope and limitations of these complexes as a catalyst in the dehydrogenation of various secondary alcohols. Furthermore, racemization of secondary alcohols by complexes **3a–e** with the aim of applying these catalysts in the dynamic kinetic resolution (DKR) of secondary alcohols is under investigation.²⁴

Experimental Section

General Procedures. All experiments were carried out under an atmosphere of dry argon using standard Schlenk techniques. All reactants and solvents were obtained from commercial suppliers and were used as received. Ru(OCOFCF₃)₂(CO)(PPh₃)₂ (**1**) was synthesized according to a literature procedure.¹²

¹H, ¹³C, and ³¹P NMR spectra were recorded on a Varian Mercury Vx 400 (400 MHz for ¹H NMR, 101 MHz for ¹³C NMR, and 162 MHz for ³¹P NMR) or on a Varian Unity Inova 500 (500 MHz for ¹H NMR, 126 MHz for ¹³C NMR, and 202 MHz for ³¹P NMR) spectrometer. ¹⁹F NMR spectra were recorded on a Varian Mercury Vx 400 spectrometer at 376 MHz. ¹H and ¹³C{¹H} NMR chemical shifts are reported in ppm downfield of tetramethylsilane. ³¹P{¹H} NMR chemical shifts are reported in ppm downfield from H₃PO₄ and are referenced to an external solution of 85% H₃PO₄ in D₂O. ¹⁹F NMR chemical shifts are referenced to internal C₆F₆ at -162.9 ppm. Abbreviations used are s, singlet; d, doublet; t, triplet; dd, double doublet; tt, triple triplet; m, multiplet; br, broad. IR spectra were recorded on a Perkin-Elmer ATR-IR Spectrum One. MALDI-TOF MS spectra were recorded on a PerSeptive Biosystems Voyager DE PRO spectrometer using *trans*-2-[3-(4-*tert*-butylphenyl)-2-methyl-2-propenylidene]malononitrile (DCTB) as a matrix. GC analyses was performed on a Shimadzu 6C-17A GC equipped with a Chrompack Chirasil-DEX CB (DF = 0.25) column and an FID. Elemental analyses were performed on a Perkin-Elmer 2400 series II CHN analyzer.

Synthesis of Ru(μ -OCO-C₂F₄-OCO)(CO)(H₂O)(PPh₃)₂]₂, **2.** A round-bottom flask was charged with RuH₂(CO)(PPh₃)₃ (2.5 g, 2.7 mmol), tetrafluorosuccinic acid (0.8 g, 4.2 mmol), and toluene (60 mL). The reaction mixture was refluxed under a flow of argon for 1 h to yield a dark yellow solution. The solvent was evaporated in vacuo, and the crude product was dissolved in CH₂Cl₂. The organic phase was treated with water (2 \times) and dried over MgSO₄. The solvent was evaporated in vacuo, and crystallization from CHCl₃/*n*-pentane yielded the product as yellow needles. Yield: 1.5 g (64%).

IR (ATR): 1971 (ν_{CO}), 1652 ($\nu_{\text{CO,acid}}$) cm⁻¹. ³¹P{¹H} NMR (CDCl₃): 40.8 (d, ²J_{PP} = 29.2 Hz, 2P), 43.6 (d, ²J_{PP} = 29.2 Hz, 2P). ¹H NMR (CDCl₃): 6.32 (br, 4H, Ru-OH₂), 7.00 (m, 12H, C₆H₅), 7.11 (m, 12H, C₆H₅), 7.31 (m, 36H, C₆H₅). ¹⁹F NMR (CDCl₃): -123.0 (br d, ²J_{FF} = 260 Hz, 2F), -120.3 (br d, ²J_{FF} = 273 Hz, 2F), -119.9 (br d, ²J_{FF} = 260 Hz, 2F), -117.7 (br d, ²J_{FF} = 273 Hz, 2F). ¹³C{¹H} NMR (CDCl₃): 128.3 (d, ³J_{CP} = 10.3 Hz, 12C, *m*-C₆H₅-P), 128.4 (d, ³J_{CP} = 10.4 Hz, 12C, *m*-C₆H₅-P), 130.2 (d, ¹J_{CP} = 48.9 Hz, 6C, *i*-C₆H₅-P), 130.5 (d, ⁴J_{CP} = 2.9 Hz, 6C, *p*-C₆H₅-P), 130.7 (d, ¹J_{CP} = 50.4 Hz, 6C, *i*-C₆H₅-P), 130.9 (d, ⁴J_{CP} = 2.7 Hz, 6C, *p*-C₆H₅-P), 134.4 (d, ²J_{CP} = 9.5 Hz,

12C, *o*-C₆H₅-P), 134.5 (d, ²J_{CP} = 10.0 Hz, 12C, *o*-C₆H₅-P), 165.87 (t, 2C, OCO), 169.01 (t, 2C, OCO), 202.70 (t, 2C, Ru-CO). MS (MALDI-TOF, matrix: DCTB): 843 [1/2M - H₂O + H⁺]⁺. Anal. Calcd for C₈₂F₈H₆₄O₁₂P₄Ru₂: C, 57.28; H, 3.75. Found: C, 57.04; H, 3.66.

Synthesis of Ru(μ -OCO-C₂F₄-OCO)(CO)(H₂O)(dpppp)]₂, **3a.** A round-bottom flask was charged with **2** (175 mg, 0.10 mmol), 1,3-bis(diphenylphosphino)propane (88 mg, 0.21 mmol), and toluene (15 mL). The reaction mixture was allowed to react for 2 h at 100 °C under a flow of argon. The solvent was evaporated in vacuo, and the crude product was obtained upon precipitation from toluene by addition of *n*-pentane. Recrystallization from CHCl₃/methanol with slow diffusion of *n*-pentane gave yellow needles. Yield: 135 mg (89%).

IR (ATR): 1984 (ν_{CO}), 1680 ($\nu_{\text{CO,acid}}$), 1625 ($\nu_{\text{CO,acid}}$) cm⁻¹. ³¹P{¹H} NMR (CDCl₃): 36.6 (d, ²J_{PP} = 42.8 Hz, 2P), 40.1 (d, ²J_{PP} = 42.8 Hz, 2P). ¹H NMR (CDCl₃): 1.76 (m, 2H), 2.17 (m, 4H), 2.41 (m, 2H), 2.78 (m, 4H), 5.52 (br, 4H, Ru-OH₂), 7.0–8.1 (C₆H₅, 40H). ¹⁹F NMR (CDCl₃): -123.6, (br d, ²J_{FF} = 173 Hz, 2F), -122.9, (br d, ²J_{FF} = 173 Hz, 2F), -118.2, (m, ²J_{FF} = 218 Hz, ³J_{FF} = 17 Hz, ³J_{FF} = 9 Hz, 2F), -117.5, (m, ²J_{FF} = 218 Hz, ³J_{FF} = 17 Hz, ³J_{FF} = 9 Hz, 2F). ¹³C{¹H} NMR (CDCl₃): 19.05 (m, 2C, P-CH₂-CH₂-), 27.06 (m, 4C, P-CH₂-CH₂-), 128.4–134.1 (aromatic, 48C), 163.98 (t, 2C, OCO), 169.97 (t, 2C, OCO), 202.93 (t, 2C, Ru-CO). MS (MALDI-TOF, matrix: DCTB): 1461 [M - 2H₂O + H⁺]⁺, 731 [1/2M - H₂O + H⁺]⁺. Anal. Calcd for C₆₄F₈H₅₆O₁₂P₄Ru₂: C, 51.41; H, 3.78. Found: C, 51.22; H, 3.62.

Synthesis of Ru(μ -OCO-C₂F₄-OCO)(CO)(H₂O)(dppb)]₂·H₂O, **3b.** A round-bottom flask was charged with **2** (176 mg, 0.10 mmol), 1,4-bis(diphenylphosphino)butane (90 mg, 0.21 mmol), and chloroform (15 mL). The reaction mixture was allowed to react for 1.5 h at 60 °C under a flow of argon. The solvent was evaporated in vacuo, and the crude product was obtained upon precipitation from chloroform by addition of *n*-pentane. Recrystallization from CHCl₃/methanol with slow diffusion of *n*-pentane gave yellow needles. Yield: 132 mg (85%).

IR (ATR): 1992 (ν_{CO}), 1968 (ν_{CO}), 1645 ($\nu_{\text{CO,acid}}$) cm⁻¹. ³¹P{¹H} NMR (CDCl₃): 41.3 (d, ²J_{PP} = 33.4 Hz, 2P), 41.7 (d, ²J_{PP} = 33.4 Hz, 2P). ¹H NMR (CDCl₃): 1.76 (m, 8H), 1.7 (br, 2H, H₂O), 2.54 (m, 2H), 2.69 (m, 4H), 2.83 (m, 2H), 6.23 (br, 4H, Ru-OH₂), 7.3–7.8 (aromatic, 40H). ¹⁹F NMR (CDCl₃): -121.2, (4F), -120.5, (br d, ²J_{FF} = 264 Hz, 2F), -118.8, (br d, ²J_{FF} = 264 Hz, 2F). ¹³C{¹H} NMR (CDCl₃): 22.92 (m, 4C, P-CH₂-CH₂-), 29.58 (m, 4C, P-CH₂-CH₂-), 128.46 (m, 4C, *m*-C₆H₅-P), 128.76 (m, 4C, *m*-C₆H₅-P), 130.40 (br, 2C, *p*-C₆H₅-P), 130.81 (br, 2C, *p*-C₆H₅-P), 130.88 (d, ¹J_{CP} = 46.3 Hz, 2C, *i*-C₆H₅-P), 130.90 (br, 4C, *p*-C₆H₅-P), 132.26 (d, ²J_{CP} = 8.5 Hz, 2C, *o*-C₆H₅-P), 132.61 (d, ¹J_{CP} = 50.3 Hz, 2C, *i*-C₆H₅-P), 132.54 (d, ¹J_{CP} = 44.3 Hz, 2C, *i*-C₆H₅-P), 132.52 (d, ²J_{CP} = 8.1 Hz, 2C, *o*-C₆H₅-P), 133.18 (d, ²J_{CP} = 8.6 Hz, 2C, *o*-C₆H₅-P), 133.92 (d, ²J_{CP} = 8.1 Hz, 2C, *o*-C₆H₅-P), 134.00 (d, ¹J_{CP} = 53.3 Hz, 2C, *i*-C₆H₅-P), 165.45 (t, ²J_{CF} = 25.6 Hz, 2C, OCO), 168.92 (t, ²J_{CF} = 26.8 Hz, 2C, OCO), 202.24 (t, ²J_{CP} = 17.6 Hz, 2C, Ru-CO). MS (MALDI-TOF, matrix: DCTB): 1489 [M - 2H₂O + H⁺]⁺, 745 [1/2M - H₂O + H⁺]⁺. Anal. Calcd for C₆₆F₈H₆₂O₁₃P₄Ru₂: C, 51.43; H, 4.06. Found: C, 51.39; H, 3.89.

Synthesis of Ru(μ -OCO-C₂F₄-OCO)(CO)(H₂O)(dpppf)]₂·H₂O, **3c.** A round-bottom flask was charged with **2** (199 mg, 0.12 mmol), 1,1'-bis(diphenylphosphino)ferrocene (147 mg, 0.27 mmol), and toluene (22 mL). The reaction mixture was allowed to react for 1 h at 100 °C under a flow of argon, resulting in an orange suspension. The crude product precipitated from the reaction mixture upon addition of *n*-pentane. Recrystallization from CHCl₃/methanol with slow diffusion of *n*-pentane gave orange crystals. Yield: 146 mg (71%).

IR (ATR): 1972 (ν_{CO}), 1651 ($\nu_{\text{CO,acid}}$) cm⁻¹. ³¹P{¹H} NMR (CDCl₃): 45.1 (d, ²J_{PP} = 30.5 Hz, 2P), 46.3 (d, ²J_{PP} = 30.5 Hz,

(24) (a) Larsson, A. L. E.; Persson, B. A.; Bäckvall, J.-E. *Angew. Chem., Int. Ed. Engl.* **1997**, *36*, 1211. (b) Pamiés, O.; Bäckvall, J.-E. *Chem. Rev.* **2003**, *103*, 3247. (c) Choi, J. H.; Choi, Y. K.; Kim, Y. H.; Park, E. S.; Kim, E. J.; Kim, M.-J.; Park, J. J. *Org. Chem.* **2004**, *69*, 1972. (d) Martin-Matute, B.; Edin, M.; Bogar, K.; Bäckvall, J.-E. *Angew. Chem., Int. Ed.* **2004**, *43*, 6535.

2P). ^1H NMR (CDCl_3): 1.86 (br, 2H, H_2O), 4.29 (m, 2H, C_5H_4), 4.33 (m, 2H, C_5H_4), 4.36 (m, 2H, C_5H_4), 4.39 (m, 2H, C_5H_4), 4.44 (m, 2H, C_5H_4), 4.53 (m, 2H, C_5H_4), 4.63 (m, 2H, C_5H_4), 4.80 (m, 2H, C_5H_4), 6.30 (br, 4H, $\text{Ru}-\text{OH}_2$), 7.2–8.9 (56H, C_6H_5). ^{19}F NMR (CDCl_3): -123.5, (br dd, $^2J_{\text{FF}} = 262$ Hz, $^3J_{\text{FF}} = 16$ Hz, 2F), -120.4, (br dd, $^2J_{\text{FF}} = 275$ Hz, $^3J_{\text{FF}} = 16$ Hz, 2F), -119.5, (br dd, $^2J_{\text{FF}} = 262$ Hz, $^3J_{\text{FF}} = 16$ Hz, 2F), -116.2, (br dd, $^2J_{\text{FF}} = 275$ Hz, $^3J_{\text{FF}} = 16$ Hz, 2F). $^{13}\text{C}\{^1\text{H}\}$ NMR (CDCl_3): 72.1–78.6 ($\text{C}_5\text{H}_4-\text{P}$, 20C), 127.9 (d, $^3J_{\text{CP}} = 10.6$ Hz, 4C, $m-\text{C}_6\text{H}_5-\text{P}$), 128.2 (d, $^3J_{\text{CP}} = 10.2$ Hz, 4C, $m-\text{C}_6\text{H}_5-\text{P}$), 128.2 (d, $^3J_{\text{CP}} = 10.4$ Hz, 4C, $m-\text{C}_6\text{H}_5-\text{P}$), 128.3 (d, $^3J_{\text{CP}} = 10.4$ Hz, 4C, $m-\text{C}_6\text{H}_5-\text{P}$), 130.2 (d, $^4J_{\text{CP}} = 2.5$ Hz, 2C, $p-\text{C}_6\text{H}_5-\text{P}$), 130.8 (d, $^4J_{\text{CP}} = 2.4$ Hz, 2C, $p-\text{C}_6\text{H}_5-\text{P}$), 130.9 (d, $^4J_{\text{CP}} = 2.4$ Hz, 2C, $p-\text{C}_6\text{H}_5-\text{P}$), 131.0 (d, $^4J_{\text{CP}} = 2.6$ Hz, 2C, $p-\text{C}_6\text{H}_5-\text{P}$), 131.0 (d, $^1J_{\text{CP}} = 52.6$ Hz, 2C, $i-\text{C}_6\text{H}_5-\text{P}$), 132.8 (d, $^1J_{\text{CP}} = 52.2$ Hz, 2C, $i-\text{C}_6\text{H}_5-\text{P}$), 133.6 (d, $^2J_{\text{CP}} = 10.1$ Hz, 4C, $o-\text{C}_6\text{H}_5-\text{P}$), 134.2 (d, $^2J_{\text{CP}} = 10.1$ Hz, 4C, $o-\text{C}_6\text{H}_5-\text{P}$), 134.3 (d, $^1J_{\text{CP}} = 54.6$ Hz, 2C, $i-\text{C}_6\text{H}_5-\text{P}$), 134.4 (d, $^2J_{\text{CP}} = 10.1$ Hz, 4C, $o-\text{C}_6\text{H}_5-\text{P}$), 134.9 (d, $^2J_{\text{CP}} = 9.7$ Hz, 4C, $o-\text{C}_6\text{H}_5-\text{P}$), 166.6 (t, $^2J_{\text{CF}} = 26.6$ Hz, 2C, OCO), 169.0 (t, $^2J_{\text{CF}} = 26.6$ Hz, 2C, OCO), 202.7 (t, $^2J_{\text{CP}} = 26.4$ Hz, 2C, Ru-CO). MS (MALDI-TOF, matrix: DCTB): 1745 [M - 2H₂O + H⁺]⁺, 873 [1/2M - H₂O + H⁺]⁺. Anal. Calcd for C₇₈F₈-Fe₂H₆₂O₁₃P₄Ru₂: C, 52.13; H, 3.48. Found: C, 52.09; H, 3.26.

Synthesis of Ru(μ -OCO-C₂F₄-OCO)(CO)(H₂O)(rac-BINAP)]₂, 3d. A 50 mL glass microwave reactor vessel (Milestone) was charged with **2** (246 mg, 0.14 mmol), *rac*-2,2'-bis(diphenylphosphino)-1,1'-binaphthalene (BINAP) (202 mg, 0.32 mmol), and toluene (30 mL). The reactor was flushed with argon. The reaction mixture was allowed to react at 180 °C for 80 min using a maximum power of 600 W. After cooling, *n*-pentane (15 mL) was added to the reaction mixture, and **3d** was subsequently obtained upon filtration and washing with *n*-pentane. Yield: 219 mg (80%).

NMR (^1H , ^{13}C , ^{19}F and ^{31}P) data are similar to those of the (*S*)-BINAP complex **3e**, indicating that the major product is the racemic complex. From $^{31}\text{P}\{^1\text{H}\}$ NMR the fraction of racemic product can be estimated as >80%. The signals for the *meso*-complex could not be resolved. IR (ATR): 1985 (ν_{CO}), 1979 (ν_{CO}), 1675 (ν_{CO}), 1667 (ν_{CO}) cm⁻¹. MS (MALDI-TOF, matrix: DCTB): 941 [1/2M - H₂O + H⁺]⁺. Anal. Calcd for C₉₈F₈H₆₈O₁₂P₄Ru₂: C, 61.44; H, 3.58. Found: C, 61.42; H, 3.34.

Synthesis of Ru(μ -OCO-C₂F₄-OCO)(CO)(H₂O)((*S*)-BINAP)]₂, 3e. A 50 mL glass microwave reactor vessel (Milestone) was charged with **2** (200 mg, 0.12 mmol), (*R*)-(+)-2,2'-bis(diphenylphosphino)-1,1'-binaphthalene (BINAP) (190 mg, 0.31 mmol), and toluene (25 mL). The reactor was flushed with argon. The reaction mixture was allowed to react at 180 °C for 40 min using a maximum power of 600 W. The solvent was evaporated in vacuo, and the crude product was obtained by precipitation from CH₂Cl₂ by addition of *n*-pentane. Recrystallization from CHCl₃ with slow diffusion of *n*-pentane gave yellow crystals. Yield: 164 mg (74%).

IR (ATR): 1977 (ν_{CO}), 1655 ($\nu_{\text{CO,acid}}$) cm⁻¹. $^{31}\text{P}\{^1\text{H}\}$ NMR (CDCl_3): 42.8 (d, $^2J_{\text{PP}} = 30.5$ Hz, 2P), 44.4 (d, $^2J_{\text{PP}} = 30.5$ Hz, 2P). ^1H NMR (CDCl_3): 6.07 (br, 4H, Ru-OH₂), 6.4–7.8 (aromatic, 64H). ^{19}F NMR (CDCl_3): -122.9 (br d, $^2J_{\text{FF}} = 256$ Hz, 2F), -122.6 (br d, $^2J_{\text{FF}} = 260$ Hz, 2F), -117.8 (br d, $^2J_{\text{FF}} = 260$ Hz, 2F), -117.4 (br d, $^2J_{\text{FF}} = 256$ Hz, 2F). $^{13}\text{C}\{^1\text{H}\}$ NMR (CDCl_3): 126–139 (aromatic, 80C), 133.25 (d, $^2J_{\text{CP}} = 11.1$ Hz, 2C, $o-\text{C}_6\text{H}_5-\text{P}$), 134.11 (d, $^2J_{\text{CP}} = 10.5$ Hz, 2C, $o-\text{C}_6\text{H}_5-\text{P}$), 135.63 (d, $^2J_{\text{CP}} = 9.4$ Hz, 2C, $o-\text{C}_6\text{H}_5-\text{P}$), 136.07 (d, $^2J_{\text{CP}} = 8.9$ Hz, 2C, $o-\text{C}_6\text{H}_5-\text{P}$), 165.3 (t, 2C, OCO), 170.2 (t, 2C, OCO), 202.3 (t, 2C, Ru-CO). MS (MALDI-TOF, matrix: DCTB): 941 [1/2M - H₂O + H⁺]⁺. Anal. Calcd for C₉₈F₈H₆₈O₁₂P₄Ru₂: C, 61.44; H, 3.58. Found: C, 61.05; H, 3.26.

Synthesis of [Ru(μ -H)(μ -OCO-C₂F₄-OCO)(CO)(rac-BINAP)]₂·3H₂O, 4d. A 100 mL flask was charged with **2** (500 mg, 0.29 mmol), *rac*-2,2'-bis(diphenylphosphino)-1,1'-binaphthalene (BINAP) (477 mg, 0.77 mmol), and *p*-xylene (25 mL). The reaction

mixture was allowed to react for 20 h at 130 °C under an argon atmosphere. ^1H NMR indicated that the reaction was not complete, and extra *rac*-2,2'-bis(diphenylphosphino)-1,1'-binaphthalene (BINAP) (390 mg, 0.63 mmol) and 20 mL of *p*-xylene were added. The reaction mixture was allowed to react for 19 h at 138 °C under an argon atmosphere. The resulting suspension was centrifuged, and the residue was used without further purification. A 50 mL flask was charged with the crude product and 20 mL of 1-phenylethanol. The reaction mixture was allowed to react for 1 h at 130 °C and then allowed to cool to room temperature. The solvent was evaporated in vacuo, and the crude product was dissolved in 20 mL of CH₂Cl₂. Addition of ethanol (30 mL) resulted in the crystallization of excess *rac*-BINAP. Filtration and subsequent concentration of the filtrate in vacuo yielded the crude product, which was further purified by precipitation from CH₂Cl₂ by addition of *n*-pentane. Yield: 332 mg (65%). **4d** was also synthesized on a small scale using the method reported for **4e**.

NMR signals for *rac*-**4d** and (*R,S*)-**4d** overlap, rendering accurate assignment impossible. As expected, the signals for *rac*-**4d** correspond to the data reported for **4e**. Selected NMR data for (*R,S*)-**4d** in CDCl₃: ^1H NMR: -10.72 (tt, 1H, Ru-*H*-Ru), -10.60 (tt, 1H, Ru-*H*-Ru), 6.6–8.1 (64H, aromatic). $^{31}\text{P}\{^1\text{H}\}$ NMR: 41.4 (m, 2P), 44.5 (m, 2P). ^{19}F NMR: -115.4 (br, 2F), -114.9 (br, 2F).

Synthesis of [Ru(μ -H)(μ -OCO-C₂F₄-OCO)(CO)((*S*)-BINAP)]₂·3H₂O, 4e. A 100 mL flask was charged with **3e** (209 mg, 0.11 mmol), 2-propanol (3.3 g, 55 mmol), and triethylamine (2.8 g, 28 mmol). The reaction mixture was allowed to react for 2 h at 25 °C under an argon atmosphere. The reaction mixture was concentrated in vacuo, and the crude product was purified by filtration over silica gel using ethyl acetate as the eluent. Yield: 136 mg (74%).

IR (ATR): 1979 (ν_{CO}), 1947 ($\nu_{\text{Ru-H}}$), 1679 ($\nu_{\text{CO,acid}}$), 1614 ($\nu_{\text{CO,acid}}$) cm⁻¹. $^{31}\text{P}\{^1\text{H}\}$ NMR (CDCl_3): 38.8 (dd, $^2J_{\text{PP}} = 36.0$ Hz, $^4J_{\text{PP}} = 26.1$ Hz, 2P), 46.4 (dd, $^2J_{\text{PP}} = 36.0$ Hz, $^4J_{\text{PP}} = 26.1$ Hz, 2P). ^1H NMR (CDCl_3): -10.38 (tt, $^2J_{\text{HP}} = 48.0$ Hz, $^2J_{\text{HP}} = 10.0$ Hz, 2H, Ru-*H*-Ru), 1.78 (br, 6H, H₂O), 6.6–8.1 (64H, aromatic). ^{19}F NMR (CDCl_3): -114.9 (br d, $^2J_{\text{FF}} = 271$ Hz, 1F), -114.4 (br d, $^2J_{\text{FF}} = 271$ Hz, 1F), -113.8 (br d, $^2J_{\text{FF}} = 271$ Hz, 1F), -113.4 (br d, $^2J_{\text{FF}} = 271$ Hz, 1F). $^{13}\text{C}\{^1\text{H}\}$ NMR (CDCl_3): 126–140 (aromatic, 88C), 161.9 (t, 1C, OCO), 164.4 (t, 1C, OCO), 203.5 (t, 2C, Ru-CO). Anal. Calcd for C₉₈F₈H₆₈O₁₂P₄Ru₂: C, 64.60; H, 4.15. Found: C, 64.40; H, 3.77.

Typical Procedure for the Dehydrogenation of 1-Phenylethanol at 130 °C. An oven-dried 40 mL Radley carousel reaction tube was charged with catalyst (0.01 mmol of **2**, **3**, or **4**, 0.02 mmol of **1**), 1-phenylethanol (5 mmol), and 1,3,5-tri-*tert*-butylbenzene (0.25 mmol). The reaction tube was placed in a 12-tube Radley reaction carousel and heated to 130 °C under an argon atmosphere in an open system. At 130 °C *p*-xylene (2 mL) was added and the reaction was stirred for several hours (the preactivation time was consequently on the order of 10 min). Small aliquots of reaction mixture were taken for GC analysis. [Due to reaction conditions (high temperature, open system) and the limited reflux ability of the carousel reactor used, loss of a few percent of substrate/product could not be avoided. The internal standard could therefore not be used for the calculation of conversions. However, no byproducts were observed or expected based on GC and ^1H NMR analysis except for a trace amount of byproducts originating from the second TFSA ligand.]

Typical Procedure for the Dehydrogenation of 1-Phenylethanol at 100 °C. A Schlenk tube was charged with catalyst (0.0025 mmol), 1-phenylethanol (0.5 mmol), 1,3,5-tri-*tert*-butylbenzene (0.025 mmol), and toluene (1 mL). The reaction mixture was heated at 100 °C for several hours under an argon atmosphere in an open system. Small aliquots of reaction mixture were taken for GC analysis.

X-ray Crystal Structure Analyses. Pertinent data for the structure determinations are given in Table 3. Data were collected

Table 3. Crystallographic Data for Crystal Structure Determinations of **2**, (*rac*)-**4d**, and (*R,S*)-**4d**

	2	(<i>rac</i>)- 4d	(<i>R,S</i>)- 4d
formula ^a	C ₈₂ H ₆₄ F ₈ O ₁₂ P ₄ Ru ₂ ·CHCl ₃	C ₉₄ H ₆₆ F ₄ O ₆ P ₄ Ru ₂	C ₉₄ H ₆₆ F ₄ O ₆ P ₄ Ru ₂
molecular weight ^a	1838.72	1693.58	1693.58
cryst syst	monoclinic	triclinic	monoclinic
space group	<i>P</i> 2 ₁ / <i>c</i> (No. 14)	<i>P</i> 1̄ (No. 2)	<i>P</i> 2 ₁ / <i>c</i> (No. 14)
<i>a</i> , Å	18.779(2)	20.4988(12)	15.8597(14)
<i>b</i> , Å	29.4780(10)	20.8765(12)	28.260(4)
<i>c</i> , Å	18.7773(10)	25.2786(15)	21.528(2)
α, deg		66.336(18)	
β, deg	118.647(10)	67.039(18)	102.80(2)
γ, deg		84.820(18)	
<i>V</i> , Å ³	9122.1(11)	9095(2)	9409.0(19)
<i>D</i> _{calc} , ^a g cm ⁻³	1.339	1.237	1.195
<i>Z</i>	4	4	4
<i>F</i> (000) ^a	3720	3448	3448
μ(Mo <i>K</i> α), ^a mm ⁻¹	0.559	0.449	0.440
cryst color	yellow	orange	orange
cryst size, mm	0.10 × 0.15 × 0.35	0.10 × 0.10 × 0.35	0.05 × 0.10 × 0.35
θ _{min} , θ _{max} , deg	0.6, 27.5	1.1, 25.3	1.2, 20.0
total data	211 111	194 246	44 353
unique data	20 806	32 942	8532
<i>R</i> _{int}	0.0804	0.1760	0.2058
<i>V</i> disordered solvent (Å ³)	1833	2329	2826
no. <i>e</i> in disordered solvent	540	754	687
no. of refined params	1009	1981	556
final <i>R</i> ₁ ^b	0.0444 [15 510 <i>I</i> > 2σ(<i>I</i>)]	0.0725 [17 850 <i>I</i> > 2σ(<i>I</i>)]	0.0991 [4539 <i>I</i> > 2σ(<i>I</i>)]
final <i>wR</i> ₂ ^c	0.1358	0.1924	0.2676
goodness of fit	1.063	0.976	1.048
<i>w</i> ⁻¹ ^d	σ ² (<i>F</i> _o ²) + (0.0844 <i>P</i>) ²	σ ² (<i>F</i> _o ²) + (0.0965 <i>P</i>) ²	σ ² (<i>F</i> _o ²) + (0.1104 <i>P</i>) ² + 30.7 <i>P</i>
min., max. Δρ, e Å ⁻³	-0.66, 0.80	-0.71, 1.35	-0.65, 0.53

^a Excluding disordered solvent contribution, including hydride atom contribution. ^b $R_1 = \sum ||F_o| - |F_c|| / \sum |F_o|$. ^c $wR_2 = [\sum [w(F_o^2 - F_c^2)^2] / \sum [w(F_o^2)^2]]^{1/2}$. ^d $P = (\text{Max}(F_o^2, 0) + 2F_c^2) / 3$.

at 150 K on a Nonius KappaCCD diffractometer on a rotating anode (graphite-monochromated Mo *K*α radiation, λ = 0.71073 Å). The unit-cell parameters were checked for the presence of higher lattice symmetry.²⁵ The structures were solved with direct methods using SHELXS86²⁶ (compound **2**) or automated Patterson and subsequent difference Fourier methods using DIRDIF99²⁷ (compounds **4d**). Refinement on *F*² was performed with SHELXL-97.²⁸ All hydrogen atoms were included on calculated positions riding on their carrier atoms. The crystal of (*rac*)-**4d** turned out to be a twin. The twin operation was a rotation of 180° around the *b*-axis (twin matrix -1 0 0, 0.159 1 -0.713, 0 0 -1) with a minor twin component of 0.1713(19). The structure was refined on detwinned intensity data. All three structures showed a large area of disordered solvent for which no satisfactory atomic model could be obtained. The contribution of the disordered solvent to the scattered intensity was taken into account with the squeeze procedure, as incorporated in PLATON.²⁹ The data set of (*R,S*)-**4d** showed a strong drop in intensity at higher diffraction angles. Data were therefore collected up to θ = 20°. To maintain a reasonable data:parameter ratio, the

carbon atoms were refined with isotropic displacement parameters. The hydride atoms in the structures of (*R,S*)-**4d** and (*rac*)-**4d** could not be unambiguously located and were therefore left out of the refined model. Neutral atom scattering factors and anomalous dispersion corrections were taken from the International Tables for Crystallography.³⁰ Validation, geometrical calculations, and illustrations were performed with PLATON.²⁹

Acknowledgment. DSM Pharma Chemicals is gratefully acknowledged for financial support. This work was supported in part (A.L.S.) by the Council for the Chemical Sciences of Netherlands Organization for Scientific Research (CW-NWO).

Supporting Information Available: Further details in CIF format on the crystal structures of complexes **2**, (*rac*)-**4d**, and (*R,S*)-**4d**, including atomic coordinates, displacement parameters, bond lengths, and bond angles, Figure S1 showing the ORTEP plot of the molecular structure of (*R,S*)-**4d**, Figure S2 showing the ³¹P-{¹H} NMR spectra of **2** at elevated temperature, and Figure S3 showing the kinetics for the dehydrogenation of 1-phenylethanol at 100 °C by catalyst **4c**. This material is available free of charge via the Internet at <http://pubs.acs.org>.

OM050789S

(30) Wilson, A. J. C., Ed. *International Tables for Crystallography, Volume C*; Kluwer Academic Publishers: Dordrecht, The Netherlands, 1992.

(25) Spek, A. L. *J. Appl. Crystallogr.* **1988**, *21*, 578.

(26) Sheldrick, G. M. *SHELXS86*, Program for crystal structure determination; University of Göttingen: Germany, 1986.

(27) Beurskens, P. T.; Admiraal, G.; Beurskens, G.; Bosman, W. P.; Garcia-Granda, S.; Gould, R. O.; Smits, J. M. M.; Smykalla, C. *The DIRDIF99 program system*, Technical Report of the Crystallography Laboratory; University of Nijmegen: The Netherlands, 1999.

(28) Sheldrick, G. M. *SHELXS-97*, Program for crystal structure refinement; University of Göttingen: Germany, 1997.

(29) Spek, A. L. *J. Appl. Crystallogr.* **2003**, *36*, 7.